J. Phys. B: At. Mol. Opt. Phys. **26** (1993) 2201–2215. Printed in the UK

Electron scattering from potassium at intermediate energies

J Mitroy†

Centre for Atomic, Molecular and Surface Physics, Murdoch University, Murdoch, WA, 6150, Australia

Received 5 January 1993, in final form 8 April 1993

Abstract. Calculations of intermediate energy electron scattering from the ground state of the potassium atom are performed using the unitarized distorted wave Born approximation. The target states (4s, 4p, 5s, 3d, 5p, 4d) of the potassium atom are calculated with a semi-empirical polarization potential added to the Hartree–Fock potential of the fixed core. Differential cross sections for elastic scattering and the 4s → 4p resonant excitation are presented and compared with experimental data. In general, the calculated cross sections exceed the experimental cross sections for large angle scattering by factors varying between two and ten. Integrated cross sections are also computed and are in agreement with experiment.

1. Introduction

In this paper an investigation of electron–potassium scattering in the intermediate energy region is presented. Unlike sodium, which has received a large amount of attention recently, studies of potassium have been relatively scarce. Apart from a seven-state (Msezane *et al* 1992) and a four-state (McCarthy *et al* 1985) close coupling calculation all previous calculations at intermediate energies use rather primitive reaction theories. This is surprising since potassium can be treated as a single-electron system and therefore should be amenable to theoretical treatment.

There are a substantial number of relatively precise differential cross section data for elastic scattering and the resonant 4s→4p excitation (Buckman *et al* 1979, Vuskovic and Srivastava 1980). The absolute errors quoted for these measurements are less than 20%. The differential cross section data of Williams and Trajmar (1977) can be regarded as being superseded by the data of Vuskovic and Srivastava. There are also some unnormalized differential cross section data for elastic scattering (McMillen 1934, Rao and Bharathi 1987).

Integrated cross sections for the 4s → 4p resonant excitation have been derived from optical excitation functions by Chen and Gallagher (1978) and Zapesochnyi *et al* (1975). These data extend from threshold to a maximum energy of about 1000 eV.

While some Born and Glauber (Walters 1973) and distorted wave calculations have been performed (Gregory and Fink 1974, Buckman *et al* 1979, Kennedy *et al* 1977) all of these calculations are essentially first order theories. The dynamical model of the collision adopted in this work, which treats coupling between the different levels to higher orders is more sophisticated than those adopted in prior studies. There are two instances of close coupling calculations. McCarthy *et al* (1985) used a four-state model (4s, 4p, 5s, 5p) to

† Permanent address: Faculty of Science, Northern Territory University, GPO BOX 40146, Casuarina, NT, 0811, Australia.

0953-4075/93/142201+15$07.50

present differential cross section data for elastic scattering and the resonant excitation at an incident energy of 54.4 eV. Msezane *et al* (1992) used a seven-state close coupling calculation to compute integrated cross sections for elastic and inelastic scattering in an energy range from 4 to 200 eV.

The electron–potassium atom collision is studied using the unitarized distorted wave Born approximation (UDWBA). In this approximation (as implemented herein) distorted waves are computed in the static (direct) potential of the potassium. Then the distorted wave Born approximation to the K matrix (not the T matrix) is computed using the residual interactions (e.g. exchange, polarization, couplings). The advantage of the UDWBA over the ordinary DWBA is that couplings between the different channels are treated correctly to all orders of perturbation theory with the restriction that all processes take place on the energy shell. The accuracy of the UDWBA as an approximation to the full solution of the close coupling equations has been studied for electron–sodium atom scattering (Bray *et al* 1989). It has been shown to give differential cross sections for elastic scattering and the resonant 3s $\rightarrow$ 3p excitation almost identical with those obtained with the full solution of the close coupling equations at sufficiently high energies. In the present calculation six states (4s, 4p, 5s, 3p, 5p, 4d) are coupled together in the UDWBA calculation.

2. Details of the calculation

One of the primary ingredients for a realistic calculation of the excitation cross sections is of course a realistic description of the target ground and excited state wavefunctions. Although neutral potassium is effectively a one-electron system, a simple Hartree–Fock (HF) model of the atomic structure does not provide a good description of the resonant 4s $\rightarrow$ 4p transition. The HF (using the length form for the matrix element) value for the oscillator strength, 1.23, exceeds the experimental value of $\sim$ 1.00 (see table 3) by more than 20%. The reason for the discrepancy lies in the fact that the pure HF model underestimates the strength of the interaction between the closed core because no consideration is given to the polarization of the core by the valence electron. This may be rectified by adding a semi-empirical polarization potential to the Hamiltonian for the calculation of the valence states of the target state wavefunctions. Reasons of consistency also dictate that polarization potentials be added to the scattering Hamiltonian.

In order to initiate the calculations we performed a Hartree–Fock calculation of the potassium atom ground state using the analytic Hartree–Fock approach. Since the published wavefunctions of Clementi and Roetti (1974) imply a Hartree–Fock wavefunction with incorrect boundary conditions at the origin these were not used. Instead, the Slater type orbital (STO) basis functions were determined by a non-linear optimization. The functional form of a normalized STO is

$$\chi(r) = [(2n)!/(2\lambda)^{2n+1}]^{1/2} r^n \exp(-\lambda r). \tag{1}$$

Since this basis set has only one basis function with $n = l$, namely $\lambda = Z/(l+1)$ the correct Hartree–Fock boundary conditions at the origin are automatically satisfied. The details of the basis functions and the non-linear and linear parameters are given in table 1. The Hartree–Fock energy for the potassium atom ground state was −599.164 68 au. This is in very good agreement with the Hartree–Fock energy (−599.164 79 au) computed with

Table 1. Specification of the target wavefunctions for potassium. The single particle orbitals are specified in terms of linear combinations of normalized Slater type orbitals. The coefficients of each orbital are tabulated under the appropriate heading. The valence 4s, 5s, 4p, 5p, 3d and 4d orbitals were computed with polarization potentials added to the K^+ core. The 4s* and 4p* orbitals are the result of an orthodox HF calculation.

n	λ	1s	2s	3s	4s	5s	4s*
1	19.000 000	0.975 684	−0.280 252	−0.092 354	−0.020 151	0.009 784	−0.017 831
3	20.652 695	0.030 179	0.003 732	0.001 168	0.000 323	−0.000 240	0.001 125
3	12.955 481	0.009 461	0.315 456	0.115 914	0.025 075	−0.011 631	0.023 342
3	8.482 349	−0.003 875	0.630 226	0.210 848	0.048 169	−0.026 258	0.036 013
3	6.685 122	0.002 515	0.112 815	0.193 187	0.044 071	−0.017 084	0.050 007
3	4.047 145	−0.000 708	0.029 763	−0.403 801	−0.098 478	0.041 667	−0.104 787
3	2.669 078	0.000 287	−0.011 818	−0.730 412	−0.183 924	0.099 116	−0.139 270
4	2.058 771	−0.000 116	0.005 773	−0.058 723	−0.006 693	−0.009 929	−0.019 305
4	1.361 408	0.000 047	−0.002 670	0.001 420	0.342 756	−0.153 543	0.259 957
4	0.830 13	−0.000 018	0.001 150	−0.000 327	0.674 838	−0.516 133	0.686 314
4	0.569 805	0.000 006	−0.000 414	−0.001 148	0.083 968	0.376 343	0.153 36
5	0.438 789	0.00	0.00	0.00	0.00	0.850 855	0.00
5	0.309 783	0.00	0.00	0.00	0.00	0.014 185	0.00

n	λ	2p	3p	4p	5p	4p*
2	9.500 000	0.665 397	−0.202 931	0.032 342	−0.018 433	0.028 755
4	13.192 057	0.055 860	−0.013 550	0.002 261	−0.001 208	0.001 719
4	8.712 067	0.334 210	−0.085 792	0.013 220	−0.007 749	0.012 566
4	5.273 478	0.050 242	0.229 495	−0.039 014	0.023 081	−0.036 936
4	3.389 831	−0.009 345	0.560 698	−0.094 634	0.052 505	−0.079 875
4	2.138 755	0.003 350	0.335 959	−0.059 811	0.037 870	−0.052 426
4	1.261 334	−0.000 815	0.008 702	0.099 275	−0.069 409	0.063 654
4	0.769 375	0.00	0.00	0.532 183	−0.303 419	0.472 055
4	0.517 936	0.00	0.00	0.456 649	−0.596 989	0.540 022
4	0.435 400	0.00	0.00	0.00	0.246 496	0.00
4	0.314 572	0.00	0.00	0.00	1.182 893	0.00

n	λ	3d	4d
3	6.333 333	0.011 997	0.009 905
5	6.274 115	0.020 741	0.017 097
5	3.623 046	0.063 179	0.051 967
5	1.876 330	0.132 910	0.108 157
5	0.929 876	0.338 644	0.263 803
5	0.533 160	0.578 397	0.358 232
5	0.374 498	0.138 462	−0.048 513
5	0.298 000	0.000 000	−0.978 674
5	0.232 000	0.000 000	−0.088 203

the numerical approach and indicates that for all practical purposes no inaccuracies are introduced by use of the STO representation.

Having determined the wavefunction for the Hartree–Fock ground state, the core (1s, 2s, 3s, 2p, 3p) orbitals were fixed and a polarization potential of the form

$$V_{\text{pol}}(r) = \frac{-\alpha_d}{2r^4}[1 - \exp(-r^6/\rho_l^2)] \tag{2}$$

was added to the Hamiltonian. The value chosen for the static dipole polarizability, α_d, of the K^+ frozen core was 5.47 a_0^3 (Opik 1967). The values of ρ_l were determined by the requirement that the computed binding energies match the experimental binding energies

(averaged for spin–orbit splitting). The values of ρ_l were 2.10, 2.09 and 2.45 a_0 respectively for $l = 0$, 1 and 2. The specifications of the valence orbitals in terms of STOs are given in table 1.

Table 2. Theoretical and experimental binding energies (in atomic units) for the low lying states of the neutral potassium atom. The total energy of the K^+ fixed core was −599.017 21 au.

Level	Experimental[a]	HF	HF + V_{pol}
4s	0.159 516	0.147 474	0.159 518
4p	0.100 176	0.095 674	0.100 181
5s	0.063 712	0.061 061	0.063 625
3d	0.061 393	0.058 242	0.061 398
5p	0.046 912	0.045 603	0.046 888
4d	0.034 684	0.032 942	0.034 607

[a] Bashkin and Stoner (1975).

The use of the polarization potential results in an immediate improvement in the binding energies listed in table 2. Binding energies for a frozen-core HF calculation, binding energies for a frozen-core HF plus polarization potential calculation, and empirical binding energies are listed. The energies obtained with the semi-empirical Hamiltonian agree with experiment with an accuracy better than 0.3% in all cases. The HF binding energies on the other hand differ from the experiment by amounts ranging from 4% to 8%. As the same core potential was used for valence states with the same l values, the semi-empirical wavefunctions are orthogonal to quite a high degree of precision; any residual overlap was removed by the Schmidt orthogonalization procedure.

Table 3. Absorption oscillator strengths for dipole transitions beween some of the low lying states of the potassium atom.

Transition	HF	HF + V_{pol}	Other
4s–4p	1.232	0.998	0.99 ± 0.04[a], 0.96 ± 0.03[b] 1.02 ± 0.02[c], 1.012[d] 0.991[e]
4s–5p	0.009 44	0.008 92	0.0089 ± 0.0010[a]
5s–4p	0.1925	0.1886	
5s–5p	1.657	1.504	
3d–4p	0.9550	0.8275	
4p–4d	0.0112	0.000 10	
3d–5p	0.1903	0.1473	
5p–4d	1.216	1.197	

[a] Ellis and Goscinsky (1974).
[b] Link (1966).
[c] Schmeider *et al* (1968).
[d] Froese Fischer (1988).
[e] Johnson *et al* (1987).

An additional test of the quality of the target wavefunctions which is particularly relevant to the scattering calculation is the evaluation of the absorption oscillator strengths between the different states. These are listed in table 3. The Hartree–Fock oscillator strengths are computed using the dipole length form of the operator and evaluated with the experimental

energy differences. For reasons of consistency a modified form for the dipole operator is used when the oscillator strengths for the polarization wavefunctions are computed. It is

$$r' = r - \frac{\alpha_d r}{r^3}[1 - \exp(-r^6/\bar{\rho}^2)]^{1/2}. \tag{3}$$

The value of $\bar{\rho}$ used in this expression was 2.10 a_0. There are substantial differences between the two sets of oscillator strengths. For instance, the oscillator strength for the resonance transition computed using the semi-empirical method is 0.998; this is 20% smaller than the HF value and in good agreement with experiment. The importance of including a polarization potential for the core when computing properties of alkali atoms, and in particular, the ability of the semi-empirical approach to reproduce the best *ab initio* calculations has been demonstrated on numerous occasions. The semi-empirical method gives oscillator stengths practically identical to the large basis multi configuration Hartree–Fock (MCHF) calculations for sodium (Muller *et al* 1984, Froese-Fischer 1976), Al^{2+} (Mitroy and Norcross 1989, Froese-Fischer 1976), and more recently Ca^+ (Mitroy *et al* 1988, Vaeck *et al* 1992). The results presented in table 3 also indicate that the present ansatz for computing the potassium wavefunctions gives accurate answers. The oscillator strength for the resonant transition is in agreement with the experimental data (Ellis and Goscinsky 1974, Link 1966, Schmeider *et al* 1968). In addition, a many body perturbation theory (Johnson *et al* 1987) and a MCHF calculation (Froese-Fischer *et al* 1988) are no more than 2% different from the present value of 0.998.

Including a correction to the dipole matrix element is analogous to including the di-electronic polarization potential in the scattering Hamiltonian, namely

$$V_{\text{diel}}(r_1, r_2) = -\alpha_d \frac{r_1 \cdot r_2}{r_1^3 r_2^3}[1 - \exp(-r_1^6/\bar{\rho}^6)]^{1/2}[1 - \exp(-r_2^6/\bar{\rho}^6)]^{1/2}. \tag{4}$$

The value of $\bar{\rho}$ does not have to be determined to a high degree of precision since most of the partial waves will be relatively insensitive to the precise value. The relevance of the di-electronic polarization potential for scattering calculations has been demonstrated in calculations of the resonant excitation of the Al^{2+} and Ca^+ ions (Mitroy *et al* 1988, Mitroy and Norcross 1989).

A succession of different calculations of increasing sophistication have been performed. All of these calculations were done using an approach based on the momentum space solution of the Lippmann–Schwinger equation. The particulars of this approach and the interrelationships of the different approximations are detailed in Bray *et al* (1989).

FBA. This is just the first Born approximation to the T-matrix element. Ordinary Hartree–Fock wavefunctions were used for the target wavefunctions.

FBAV. This calculation is quite similar to the FBA calculation. The target wavefunctions were calculated by adding the polarization potential to the Hartree–Fock potential. In addition, the di-electronic polarization potential is included in the evaluation of the first Born matrix element.

UBA. The unitarized Born approximation is just the Born approximation to the K-matrix elements. These calculations utilize the wavefunctions computed with the core polarization potential. Calculations involvig two coupled states (UBA2, including 4s and 4p) and six coupled states (UBA6, including 4s, 4p, 5s, 3d, 5p and 4d) were done. The exchange and polarization potentials (equations (2) and (4)) were included when the K-matrix was evaluated. The UBA calculation was explicitly performed for partial waves with $J \leqslant 100$. For $J > 100$ the first Born approximation (i.e. FBAV) was used.

UDWBA. The unitarized distorted-wave Born approximation is just the distorted wave Born approximation to the K matrix. Calculations involving six coupled states (4s, 4p, 5s, 3d, 5p and 4d) were done. The distorting potential was just the static potential of the potassium ground state (minus exchange). The exchange interaction and polarization potentials (equations (2) and (4)) were included when the K-matrix elements were computed. For $20 < J \leqslant 100$, the UDWBA T-matrix elements were replaced by the UBA6 T-matrix elements since there was very little difference between the T-matrix elements for high J partial waves. For $J > 100$ the first Born approximation (i.e. FBAV) was used.

Some remarks need to be addressed regarding the completeness of the partial wave sum, especially in reference to the resonance 4s $\rightarrow$ 4p transition. Although the partial wave sum was carried up to $J = 100$ at all energies, this was not sufficient to obtain converged integrated and differential cross sections for the 4s $\rightarrow$ 4p excitation. For instance, at 54.4 eV the partial wave sum from $J = 0$ to $J = 100$ gives a value of 29.94 πa_0^2 for the integrated cross section. A simple power series extrapolation of the partial wave sum yields a cross section of 31.38 πa_0^2. However, this procedure does not give correct cross sections at higher energies. At 200 eV, extrapolation of the power series yields a cross section of 11.72 πa_0^2 which is some 8% smaller than the actual cross section (12.59 πa_0^2).

In the present calculation the integral cross sections are obtained by integrating the differential cross section rather than performing the partial wave sum. By keeping track of the individual partial wave Born matrix elements, the partial wave sum for the T matrix can be completed using the identity

$$T = V + \sum_J (T_J - V_J) \tag{5}$$

since the exact expression for the V-matrix element is easily computed (McCarthy and Stelbovics 1983).

3. Cross sections for elastic scattering

Experimental and theoretical differential cross sections for elastic scattering from potassium atoms are shown in figures 1 and 2. The two sets of data plotted in figure 1(a) were taken at slightly different incident energies. The data of Buckman *et al* (1979, hereafter abbreviated as BNT) were taken at 54.4 eV, the data of Vuskovic and Srivastava (1980, hereafter abbreviated as VS) were taken at 60 eV. The present calculations indicate that the differences between the 54.4 and 60 eV cross sections should be minor (less than 15% at most angles), and that the 60 eV cross section should be smaller at the secondary maxima. Certainly the relatively large discrepancy between the data of BNT and VS would not seem to be attributable to the energy difference, rather it would seem to be a genuine conflict between the two sets of data.

Apart from the present UDWBA cross section, the only other theoretical cross sections shown in figures 1 and 2 come from the four-state close coupling calculation of McCarthy *et al* (1985). BNT compared their elastic scattering data with an optical model calculation. However, crucial details of the calculation, such as average excitation energies for each shell are not specified. Since the exact particulars of this calculation are unknown, any comparison with this model would be meaningless (e.g. were parameters set to reproduce the experimental ionization cross section, or were they set to maximize agreement with the differential cross section?).

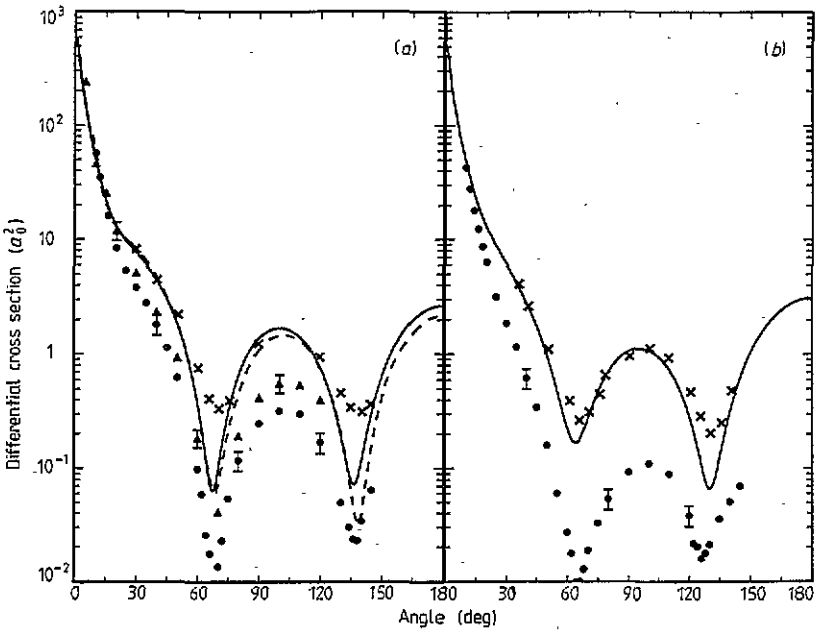

Figure 1. Differential cross sections (in units of a_0^2 sr^{-1}) for elastic scattering from the potassium ground state at energies of 54.4 (*a*) and 75 eV (*b*). Full circles (●) denote the data of BNT, full triangles (▲) denote the data of VS (at an energy of 60 eV) and crosses (×) denote the data of McMillen. The full curve (——) is the present UDWBA calculation while the broken curve (– – –) is by McCarthy *et al* (1985).

The comparison between experiment and theory exhibits two universal features. The UDWBA cross section does a reasonable job of predicting the angular position of the minima and secondary maximum in the cross section. Second, experimental cross sections are substantially smaller in magnitude than the UDWBA cross section for large angle scattering at all impact energies. For instance the ratio, $\sigma_{th}(\theta)/\sigma_{exp}(\theta)$ at the secondary cross section maximum ranges from 2 to 10 at impact energies ranging from 54.4 to 200 eV. However, it must be remarked that irregularities appear to exist in the experimental data. For instance the value of the UDWBA cross section at the secondary maxima decreases monotonically $1.682 \rightarrow 1.120 \rightarrow 0.734$ a_0^2 sr^{-1} as the energy changes from $54.4 \rightarrow 75 \rightarrow 100$ eV. In contrast, the data of BNT show a variation ($0.319 \rightarrow 0.111 \rightarrow 0.309$ a_0^2 sr^{-1}) which is certainly not smooth. To further confuse the issue, the secondary maximum of the VS data is about 0.55 a_0^2 sr^{-1} at an energy of 60 eV.

The UDWBA calculation can also be contrasted with the relatively old cross section data of McMillen (1934) in figures 1 and 2. The data have been normalized to roughly match the UDWBA calculation at the smallest angle (e.g. $\sim 30\%$). Apart from a tendency for the cross section minima to be too shallow (presumably due to poorer angular resolution) the agreement between these data and experiment is uniformly good. While the fact that the McMillen cross section is not an absolute measurement introduces a degree of ambiguity into any comparison, it is clear that the present UDWBA calculation provides a closer fit to the shape of the McMillen cross section than do the data of BNT.

The present calculation (at 54.4 eV) compare well with the previous four-state close coupling calculation of McCarthy *et al* (1985). This supports the contention (Bray *et al*

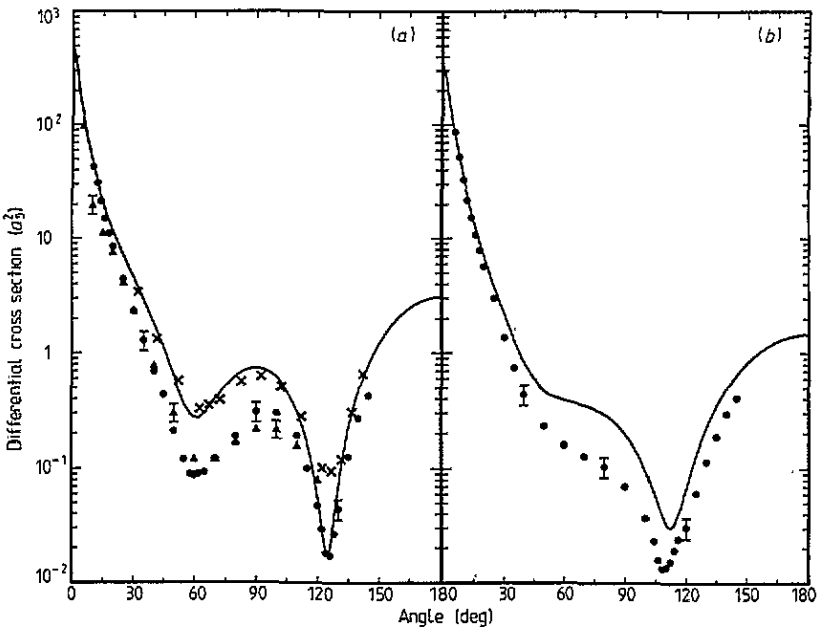

Figure 2. Differential cross sections (in units of a_0^2 sr^{-1} for elastic scattering from the potassium ground state at energies of 100 (*a*) and 200 (*b*) eV. Full circles (●) denote the data of BNT, full triangles (▲) denote the data of VS and crosses (×) denote the data of McMillen. The full curve (——) is the present UDWBA calculation.

1989) that the UDWBA is an excellent working approximation to a close coupling calculation at sufficiently high energies.

Integrated cross sections for elastic scattering are listed in table 4. These demonstrate the importance of including distortion effects in any realistic description of elastic scattering. The UBA6 cross sections are significantly smaller than the UDWBA cross sections at all energies. Comparison with the seven-state close coupling calculation (abbreviated hereafter as 7CC) of Msezane *et al* (1991) is more problematic. While there are differences in the description of the atomic structure and scattering calculation, these are not sufficient to explain the large differences between the cross sections. A discussion of the possible reasons for these differences is postponed to the next section.

Table 4. Total cross sections (in πa_0^2) for elastic scattering from the ground state of the potassium atom.

	Energy (eV)				
Model	54.42	60	75	100	200
UBA6	7.445	7.244	6.634	5.745	3.867
UDWBA6	12.04	11.49	10.28	8.814	5.932
7CC[a]		11.50		8.190	4.950

[a] Msezane *et al* (1992).

4. Cross sections for the resonant excitation

The differential cross sections for the 4s → 4p excitation were computed at incident energies of 54.4, 75, 100 and 200 eV. The small angle differential cross section data are depicted in figures 3 and 4 as generalized oscillator strengths (GOS). The data of VS depicted in figure 3(*a*) were taken at an energy of 60 eV. The GOS and not the differential cross section is depicted so that only dynamical, and not kinematic information is presented. The apparent GOS for both the UDWBA and FBAV cross sections are calculated according to the formula

$$g(K^2) = \frac{E_{if}k_i}{2k_f}K^2\frac{d\sigma}{d\Omega}. \tag{6}$$

In the above expression E_{if} is the 4s–4p energy difference, k_i is the incident momentum, k_f is the final momentum and $K(=|k_i - k_f|)$ is the momentum transfer. The apparent GOS computed from the FBAV cross section will be referred to as g_{FBAV}, while that computed from the UDWBA cross section will be called g_{UDWBA}.

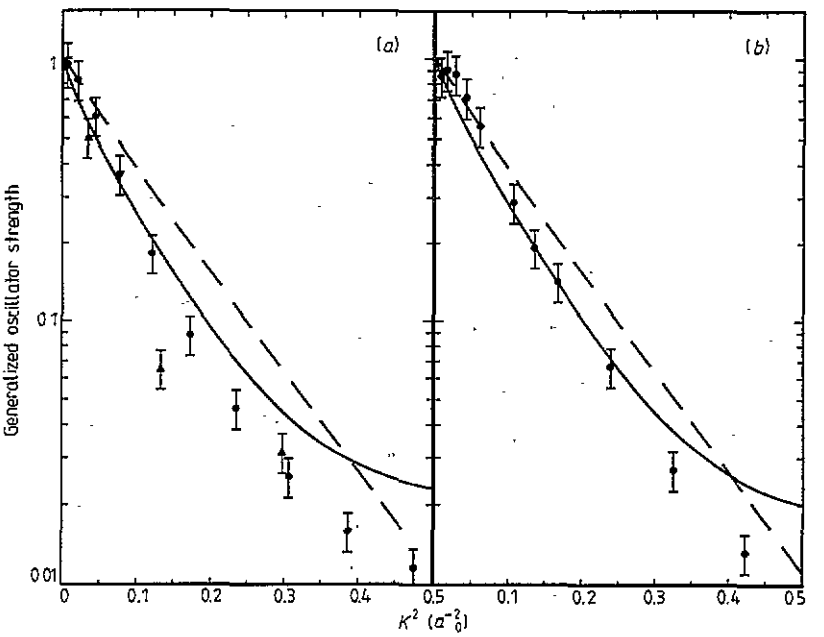

Figure 3. The generalized oscillator strength for the resonant 4s → 4p transition of the potassium atom as a function of K^2 (a_0^{-2}). Generalized oscillator strengths are shown at energies of 54.4 (*a*) and 75 eV (*b*). The data of BNT are shown as full circles (●) and the data of VS (at an energy of 60) depicted as full triangles (▲). The UDWBA calculation is depicted as a full curve (——) and the FBAV calculation is depicted as a broken curve (– – –).

As expected, the GOS for the FBAV calculation, g_{FBAV} is essentially the same at all energies. The g_{UDWBA} has two characteristic features, first, a visual inspection indicates that for all practical purposes, Lassettre's theorem (Lassettre *et al* 1969) seems to be OK, i.e. the g_{FBAV} and g_{UDWBA} converge to the same optical oscillator strength at all energies. A more detailed examination of g_{UDWBA} revealed that Lassettre's theorem is obeyed to a

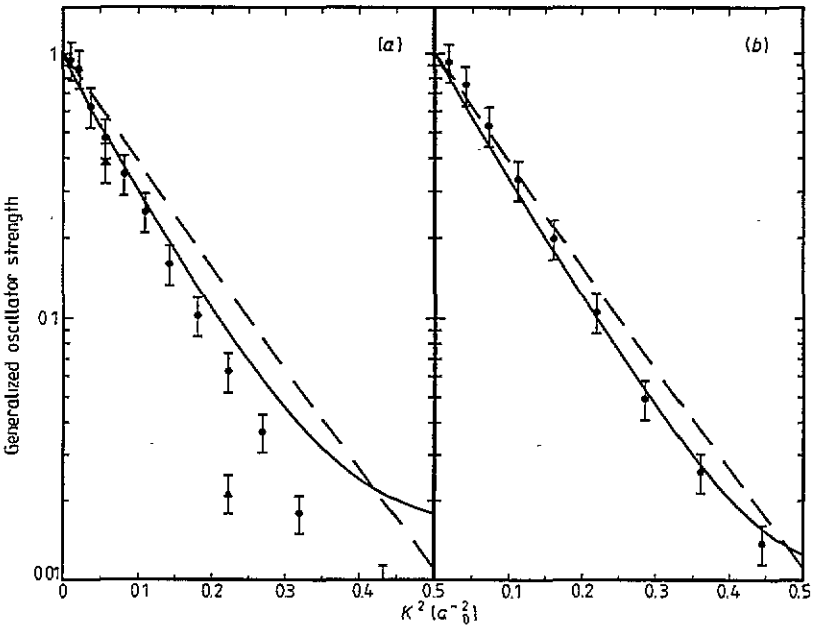

Figure 4. The generalized oscillator strength for the resonant 4s → 4p transition of the potassium atom as a function of K^2 (a_0^{-2}). Generalized oscillator strengths are shown at energies of 100 (*a*) and 200 eV (*b*). The data of BNT are shown as full circles (●) and the data of VS depicted as full triangles (▲). The UDWBA calculation is depicted as a full curve (——) and the FBAV calculation is depicted as a broken curve (– – –).

precision of better than 1% across the present energy range. At lower energies, however, the validity of this procedure is questionable (Bonham and Goruganthu 1986, Mitroy 1987).

The present g_{UDWBA} and the experimental data of BNT are in reasonable agreement for most values of K^2. Only at the larger values of K^2 does g_{UDWBA} deviate from the experimental data in any systematic manner. Mention must be made of the unusual nature of the BNT data at 75 eV. As K^2 decreases from 0.0156 to 0.0073 a_0^{-2}, the GOS decreases from 0.9073 to 0.8614. This is probably an experimental artefact resulting from the extreme difficulty of measuring the differential cross section at 2° and 3°.

Second, for values of K^2 between 0.0 and 0.4 a_0^{-2} the g_{UDWBA} is smaller than g_{FBAV}. This is probably caused by the loss of flux from the 4s–4p channel into the elastic channel (e.g. the 4s → 4p → 4s virtual excitation). For values of K^2 greater than 0.5 a_0^{-2} g_{UDWBA} starts to become larger than g_{FBAV} and also starts to diverge from the experimental data. At these larger values of K^2 a two-step process starts to contribute to the T matrix. Small angle inelastic scattering is preceded (or followed) by a large angle elastic collision with the core.

The differential cross section for the UDWBA is compared with the data of BNT and VS at 54.4 eV (60 eV for VS) and 100 eV in figure 5. Once again, the UDWBA reproduces the angular position of the minima and secondary maximum in the cross section. However, the magnitude of the cross section is considerably larger than the experimental data for scattering angles larger than 30°. The comparison with the four-state close coupling calculation of McCarthy *et al* (1985) reveals distinctions between the two calculations which are larger than those that occurred for elastic scattering. Since the 4p level is expected to couple strongly with the 3d level (which was not included in the McCarthy calculation) it is not

clear what aspects of the differences are due to the different reaction theory as opposed to the different channel space.

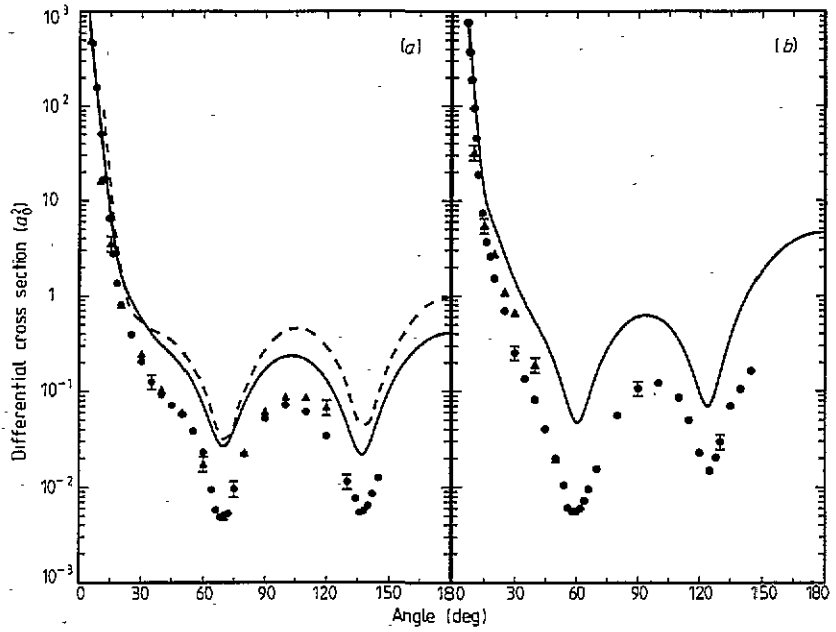

Figure 5. Differential cross sections (in units of a_0^2 sr^{-1}) for the electron impact excitation of the resonant 4s → 4p transition of the atom at energies of 54.4 (*a*) and 100 (*b*) eV. The data and curve at 100 eV are multiplied by a factor of 10. Full circles (●) denote the data of BNT while full triangles (▲) denote the data of VS (at an energy of 60 eV). The full curve (——) is the present UDWBA calculation while the broken curve (– – –) is by McCarthy *et al* (1985).

Integrated cross sections for the 4s → 4p transition are listed in table 5. A systematic trend in the cross sections is apparent when the different approximations are compared with each other. As the reaction theory becomes more realistic, the cross section decreases and conforms more closely to the experimental data. The importance of using the semi-empirical Hamiltonian for the structure and scattering calculation is clearly shown in the 20% difference between the FBAV and FBA cross sections. Similarly the importance of having a unitarized theory is shown in the 12% difference between the UBA6 and FBAV cross section at 54.4 eV. The importance of having a unitarized theory is not so important as the energy increases, at 200 eV the UBA6 and FBAV cross sections differ by less than 3%. Comparisons with the 7CC calculation of Msezane *et al* (1992) must take into account the different methods used to handle the higher partial waves which dominate the cross section. This is especially true at 200 eV, the partial wave sum to $J = 24$ yields an integrated cross section of only 1.67 πa_0^2, i.e. only 12% of the actual cross section. Msezane *et al* (1992) solve the CC equations up to a maximum J of 24, and then use the Bethe approximation to implicitly sum over the higher partial waves. The Bethe approximation is not sufficiently accurate for partial waves as low as 24. The inclusion of on-shell couplings between the different levels, as done in the UBA, leads to partial cross sections that can be different from the Bethe partial cross section by 20%.

Table 5. Total cross sections (in πa_0^2) for the resonant 4s $\rightarrow$ 4p transition in neutral potassium. Cascade corrections are not included in the theoretical data except where specified (UDWBA + cascade). The cross section of CG has contributions from excitations to higher levels which decay to the 4p level, and the present UDWBA cross section has been used to derive a set of cascade corrected cross sections (CG*). The BNT and ZPA cross sections do not include cascade contributions.

	Energy (eV)				
Model	54.42	60	75	100	200
			Theory		
FBA	42.43	39.41	33.22	26.54	15.24
FBAV	35.27	32.74	27.57	21.98	12.59
UBA2	33.36	31.19	26.54	21.40	12.41
UBA6	31.38	29.48	25.39	20.71	12.27
UDWBA	31.40	29.50	25.40	20.72	12.23
UDWBA + cascade	35.78	33.46	28.43	23.11	13.40
7CC[a]		25.51		18.21	12.00
			Experiment		
ZPA	34.4 ± 2.8		26.3 ± 2.1	21.7 ± 1.7	13.1 ± 1.1
BNT	36.7 ± 6.2		27.7 ± 4.7	21.4 ± 3.6	12.0 ± 2.0
CG	32.4 ± 1.9	30.6 ± 1.8	26.5 ± 1.6	21.8 ± 1.3	13.0 ± 0.8
CG*	27.0	26.6	23.5	19.4	11.8

[a] Msezane *et al* (1992).

Comparison of the computed integral cross section of BNT with the present cross section reveals an anomalous result. From figure 4(*b*) it is clear that at the smallest angles the differential cross section of BNT at 200 eV is larger than the present UDWBA cross section. However, the BNT integrated cross section of $12.0 \pm 2.0\ \pi a_0^2$ is smaller than the present value of $12.7\ \pi a_0^2$. Since the dominant contribution to the integrated cross section comes from small angles it is difficult to reconcile these two results. One possible explanation would be that the step size used in the integration of the BNT differential cross section was too large, for instance a step size of 1° leads to an integrated cross section which is more than 20% too small. While VS also report integrated cross sections for elastic and inelastic scattering the extent to which this information actually represents experimental data is questionable. The VS cross sections rely to a very large extent on extrapolations to 0° which provide the dominant contribution to the cross section.

The cross section data of Chen and Gallagher (1978) (abbreviated as CG) were derived from an optical excitation function, therefore transitions to levels of the potassium atom which cascade into the 4p level via photon transitions from higher levels also have to be taken into consideration. The excitation cross sections for the 5s and 3d levels must be added to the 4p cross section for a reliable comparison with the Chen and Gallagher cross section. Since the 5p and 4d levels can decay to the ground state via transition sequences (5p $\rightarrow$ 4s, 4d $\rightarrow$ 5p $\rightarrow$ 4s) not involving the 4p level, the cross sections for these levels must be multiplied by the appropriate branching fraction before being added to the 4p cross section. The branching ratios were computed using the oscillator strength calculated in this paper and detailed in table 3. Under these circumstances, the cross section becomes

$$\sigma = \sigma_{4p} + \sigma_{5s} + \sigma_{3d} + 0.801\sigma_{5p} + 0.799\sigma_{4d}.$$

Adding the cascade contributions to the cross section for direct excitation of the 4p level increases the apparent size of the UDWBA cross section by 9–14%. The comparison of the

cascade corrected UDWBA cross section with the data of CG gives reasonable agreement. The discrepancies that exist are no larger than 10% and are biggest at the lower energies.

It is possible to make cascade corrections to the data of Chen and Gallagher by subtracting the UDWBA cross sections for higher excitations from their apparent cross section. This subtraction is reported in the row labelled CG* in table 5 and it is clear that the Chen and Gallagher cross section is smaller than the UDWBA cross section.

The cross section of Zapesochnyi *et al* (1975) (abbreviated as ZPA) was derived from an optical excitation function. However, they also measure optical excitation functions for a number of higher levels and so were able to perform the cascade correction. The ZPA data listed in table 5 are taken from a digitization of a published curve. The UDWBA cross section is generally smaller than the ZPA cross section, but still within experimental uncertainties.

5. Other excitation cross sections

Integrated cross sections for excitation of the 5s, 3d, 5p and 4d levels are detailed in table 6. Excitations of these states are not dominated to the same extent by long range interactions. Hence a larger contribution to the cross section comes from the low partial waves where distortion effects are important. Therefore it is expected that the UBA6 or FBAV cross sections will not converge to the UDWBA cross sections as rapidly as they did for the 4s → 4p transition.

Table 6. Total cross sections (in πa_0^2) for excitation of the 5s, 3d, 5p and 4d levels of the potassium atom.

	Energy (eV)				
Model	54.42	60	75	100	200
			4s → 5s		
FBAV	0.762	0.693	0.558	0.420	0.212
UBA6	0.513	0.477	0.403	0.322	0.179
UDWBA	0.603	0.564	0.478	0.379	0.204
7CC[a]		0.702		0.301	0.122
			4s → 3d		
FBAV	2.577	2.343	1.882	1.417	0.713
UBA6	2.869	2.574	2.014	1.475	0.708
UDWBA	2.931	2.640	2.081	1.534	0.736
7CC[a]		2.310		1.420	0.820
			4s → 5p		
FBAV	0.537	0.491	0.400	0.307	0.162
UBA6	0.561	0.516	0.423	0.325	0.168
UDWBA	0.684	0.630	0.516	0.392	0.191
7CC[a]		0.704		0.431	0.298
			4s → 4d		
FBAV	0.347	0.315	0.253	0.189	0.0948
UBA6	0.342	0.308	0.245	0.183	0.0917
UDWBA	0.372	0.338	0.271	0.202	0.0989
7CC[a]		0.354		0.225	0.110

[a] Msezane *et al* (1992).

This is clearly apparent in table 6. For the 4s → 5p excitation, the UDWBA cross section is more than 10% larger than the UBA6 cross section at 200 eV. This feature also occurs for the other excitations, the UBA6 and UDWBA cross sections differ by some 5–10% at the highest energy considered, namely 200 eV.

The comparison with the 7CC calculations of Msezane *et al* (1992) reveals no tendency for the UDWBA and 7CC cross sections to approach each other as the energy is increased. However, as mentioned earlier the problem of correctly computing the cross sections for the higher partial waves becomes more important as the energy is increased. At the highest energy of 200 eV, the partial wave cross sections from $J = 0$–24 account for only 40% and 60% of the cross section for excitation of 3d and 4d levels respectively. Msezane *et al* do not specify how they compute the necessary correction to the cross section for non-dipole transitions, if indeed any correction is incorporated. The simplest method of correction, and one that is commonly adopted, is to assume the partial cross sections scale like a power series. An examination of the partial cross sections of the present calculations revealed that methods based on this approach do not give reliable answers.

6. Conclusions

In this paper we present a series of calculations of electron scattering from neutral potassium using a six-state (4s, 4p, 5s, 3d, 5p, 4d) UDWBA model. Although our reaction theory is a variant of the distorted wave model, it is probably the most accurate distorted wave model that can be constructed and gives results very similar to a close coupling calculation with the same set of coupled levels

Total cross sections for the 4s → 4p excitation are in reasonable agreement with experiment. The present cross section is about 10% smaller than the cross section of Zapesochnyi *et al* (1975) and some 10% larger than the cascade-corrected cross section of Chen and Gallagher (1978).

There are a number of instances of large discrepancies between theoretical and experimental differential cross section data at all energies between 54.4 and 200 eV. The UDWBA cross sections are consistently larger than the experimental cross sections. This situation is equally true for elastic scattering and the resonant 4s → 4p excitation. In many respects, the situation is similar to electron sodium scattering where similar discrepancies also exist (Mitroy *et al* 1987).

While it would be premature at this stage to ascribe all of the discrepancies to either experimental or theoretical inadequacies, there are a number of instances where irregularities are present in the experimental data. In these situations the reliability of the data should not be taken with uncritical acceptance. Two examples of such situations are, first the large angle elastic cross section of BNT at 75 eV, and second the GOS of VOS at 60 eV.

However, there are refinements which could be made to the theoretical model which could lead to reductions in the discrepancies between theory and experiment. For instance, Q-space optical potentials allowing for ionization from the valence and core orbitals could be incorporated into the calculation. Experience with sodium (Konavalov 1992, Bray *et al* 1991, Mitroy 1991) showed that the inclusion of the continuum resulted in the secondary maxima dropping by some 50% at 54 eV. However, at energies of 100 eV or greater, the inclusion of the continuum resulted in the magnitude of the secondary cross section maxima changing by a relatively small amount.

While the inclusion of the continuum would almost certainly lead to the differential cross sections for potassium becoming smaller in magnitude at backward angles, the magnitude of

the reduction remains an open question. A reduction by an amount similar to that occurring for sodium would result in substantially improved agreement at 54.4 eV, but discrepancies would still remain at higher energies. The inclusion of the continuum should also result in the integrated cross section for the 4s → 4p excitation dropping by about 5–10%, in which case theory would favour the cross section of Chen and Gallagher (1978) at the expense of Zapesochnyi *et al* (1975).

Acknowledgments

The calculations were performed using the research MicroVAX at the NTU Computer Services centre.

References

Bashkin S and Stoner J O 1975 *Atomic Energy Levels and Grotrian Diagrams* vol II (Amsterdam: North-Holland)
Bonham R A and Goruganthu R R 1986 *J. Chem. Phys.* 84 3068
Bray I, Konovalov D A and McCarthy I E 1991 *Phys. Rev.* A **44** 7830
Bray I, McCarthy I E, Mitroy J and Ratnavelu K 1989 *Phys. Rev.* A **39** 4998
Buckman S J, Noble C J and Teubner P J O 1979 *J. Phys. B: At. Mol. Phys.* **12** 3077
Chen S T and Gallagher A C 1978 *Phys. Rev.* A **17** 551
Clementi E and Roetti C A 1974 *At. Nucl. Data Tables* **14** 177
Ellis P G and Goscinsky O 1974 *Phys. Scr.* **9** 104
Froese Fischer C 1976 *Can. J. Phys.* **54** 1465
—— 1988 *Nucl. Instrum. Methods* B **31** 265
Gregory D and Fink M 1974 *At. Nucl. Data Tables* **14** 39
Johnson W R, Idrees M and Sapirstein J 1987 *Phys. Rev.* A **35** 3218
Kennedy J V, Myerscough V P and McDowell M R C 1977 *J. Phys. B: At. Mol. Phys.* **10** 3759
Konovalov D A 1992 *PhD Thesis* Flinders University (unpublished)
Lassettre E N, Skerbele A and Dillon M A 1969 *J. Chem. Phys.* **50** 1829
Link J K 1966 *J. Opt. Soc. Am.* **56** 1195
McCarthy I E, Mitroy J and Stelbovics A T 1985 *J. Phys. B: At. Mol. Phys.* **18** 2509
McCarthy I E and Stelbovics A T 1983 *Phys. Rev.* A **28** 2693
McMillen J H 1934 *Phys. Rev.* **46** 983
Mitroy J 1987 *Phys. Rev.* A **35** 4434
—— 1991 unpublished
Mitroy J, Griffin D C, Norcross D W and Pindzola M S 1988 *Phys. Rev.* A **38** 3339
Mitroy J, McCarthy I E and Stelbovics A T 1987 *J. Phys. B: At. Mol. Phys.* **20** 4827
Mitroy J and Norcross D W 1989 *Phys. Rev.* A **39** 537
Msezane A Z, Awuah P, Hiamang S and Allotey F K A 1992 *Phys. Rev.* A **46** 6949
Muller W, Flesch J and Meyer W 1984 *J. Chem. Phys.* **80** 3297
Opik U 1967 *Proc. Phys. Soc.* **92** 566
Rao M V S and Bharathi S M 1987 *J. Phys. B: At. Mol. Phys.* **20** 1081
Schmeider R W, Lurio A and Happer W 1968 *Phys. Rev.* **173** 76
Vaeck N, Godefroid M and Froese-Fischer C 1992 *Phys. Rev.* A **46** 3404
Vuskovic L and Srivastava S K 1980 *J. Phys. B: At. Mol. Phys.* **13** 4849
Walters H R 1973 *J. Phys. B: At. Mol. Phys.* **6** 1003
Williams W and Trajmar S 1977 *J. Phys. B: At. Mol. Phys.* **10** 1955
Zapesochnyi I P, Postoi E N and Aleksakhin I S 1975 *Sov. Phys.–JETP* **41** 865